Applied Energy 88 (2011) 4952–4959

Contents lists available at ScienceDirect

Applied Energy

journal homepage: www.elsevier.com/locate/apenergy

Behavior of a 300 kW_{th} regenerative multi-burner flameless oxidation furnace

E.-S. Cho [a,*], B. Danon [a,b], W. de Jong [a], D.J.E.M. Roekaerts [a,b]

[a] Process & Energy, 3mE, Delft University of Technology, The Netherlands
[b] Multi-Scale Physics, Applied Sciences, Delft University of Technology, The Netherlands

ARTICLE INFO

Article history:
Received 7 April 2011
Received in revised form 15 June 2011
Accepted 23 June 2011
Available online 3 August 2011

Keywords:
Flameless oxidation
Cycle time
Heat balance
Temperature uniformity
Emissions

ABSTRACT

The behavior of heat transfer and emissions in a semi-industrial 300 kW_{th} natural gas fired furnace with three pairs of regenerative flameless oxidation burners was studied. The furnace offers unique possibilities for varying burner positions and firing modes (parallel and staggered). The operational behavior of two burner configurations have been compared regarding emissions (NO, CO) and temperature uniformity, for both parallel and staggered firing mode. Additionally, the flue gas O_2 percentage (excess air ratio) and the cycle time have been varied. Parallel firing mode results in a higher temperature uniformity ratio in the furnace and in a lower NO emission. CO emission did not vary much between parallel and staggered mode.

1. Introduction

Energy efficiency and clean combustion are two main issues in fossil fuel utilization. Control of nitrogen oxides (NO_x) has been a major issue in designing combustion systems, since NO_x plays a key role in acid rain formation and the generation of photochemical smog [1]. Flameless Oxidation (FLOX™) [2], also known as High Temperature Air Combustion (HiTAC) [3,4], Moderate and Intensive Low oxygen Dilution (MILD) combustion [5,6] or Colorless Distributed Combustion (CDC) [7] is a promising combustion technology among various techniques [8] capable of accomplishing high efficiency and low emissions. It is based on delayed mixing of fuel and oxidizer and high flue gas recirculation in the flame zone. High momentum injection of the separated fuel and air flows entrain the flue gas through internal recirculation, thus diluting the oxygen concentration in the combustion zone [9]. This leads to a more distributed heat release rate of the chemical energy, avoiding a high peak temperature (hot spot) and reducing the thermal formation of NO_x [10]. Combined with high preheat temperature of the combustion air, this combustion technique also achieves a high efficiency. Recently, the concept of flameless combustion has been also applied in gas turbine environments [7,11].

In earlier studies, flameless oxidation has been investigated in small setups to evaluate the characteristics of the turbulent flame temperature and structure using laser measurement techniques, such as Rayleigh scattering and Laser Induced Fluorescence [12,13]. Szegö et al. tested 20kW_{th} single MILD combustion burner to evaluate the stability criteria and visualize the flame [14].

A furnace of one pair of NFK-HRS-DL4 regenerative burners has been investigated at the IFRF research station in the Netherlands [15]. The maximum thermal input is 1000 kW_{th} firing Dutch natural gas or Coke Oven Gas (COG). The experimental dataset can support the development and validation of numerical simulations.

Regarding multi-burner system, a 200 kW_{th} HiTAC furnace has been studied at KTH, Sweden. In the furnace two pairs of NFK-HRS-DF regenerative burners are fired.

Yang et al. [16] numerically investigated a two-flame high-cycle regenerative system. Also, the characteristics of flame interaction has experimentally studied in this two-flame regenerative burning system [17] varying the firing mode (parallel, staggered and counter firing). Danon et al. [18] performed both experimental and numerical studied of the furnace.

A slab reheating furnace with four pairs of regenerative burners was tested at the NKK Corporation in Japan. The total power is 2919 kW_{th} and the moving slab used as a heat sink. The experimental results compared with numerical simulation [19].

In all these studies, flameless combustion systems with one or multiple burner pairs are investigated. It is important to extend the present knowledge with furnaces with multiple burners varying burner configuration. The interaction between jets from different burners and relative position of firing and regenerating burners may play an important role. The system studied here has three regenerative burner pairs. Furthermore, in this system it is possible to do many different burner arrangements, with different distances between the burners or between the burners and the cooling tubes.

* Corresponding author. Tel.: +31 15 278 5542; fax: +31 15 278 2460.
E-mail address: e.s.cho@tudelft.nl (E.-S. Cho).

0306-2619/$ - see front matter © 2011 Elsevier Ltd. All rights reserved.
doi:10.1016/j.apenergy.2011.06.039

In this way unique study on flameless oxidation in multi-burner configuration is possible.

In this study the fundamental behavior of the multi-burner furnace at Delft University of Technology is presented. In the first place, the transition from flame to flameless mode is demonstrated in this furnace. Then, besides a detailed evaluation of the mass and heat balance, the interaction between temperature fluctuations, exhaust gas O_2 and emissions are investigated for two different burner configurations. Furthermore, the impact of the burner firing modes is studied.

2. Experimental setup

Fig. 1 shows a schematic diagram of the multi-burner furnace. The furnace consists of three pairs of regenerative FLOX™ burners; three burners are firing simultaneously, while the other three burners are regenerating. After a preset time interval, i.e. the cycle time, all the burners switch from firing to regenerating mode, and vice versa. Each burner has a rated thermal power of 100 kW_{th}, thus 300 kW_{th} in total.

The furnace has inner dimensions of 1500 × 1500 × 1850 mm (length × width × height). The insulation consists of three layers of ceramic bricks, together 300 mm thick. During the experiments the temperature in the furnace was measured at various locations with S-type thermocouples. One of those thermocouples, installed in the middle of one of the side walls of the furnace, was determined to characterize the furnace temperature. Also, the temperature of the preheated air (regenerator temperature) was measured in two burners (one burner pair). The fuel and combustion air flow rates are measured by orifice plate differential pressure meters (Kalinsky Sensor Elektronik, DS2). The combustion air flow rate is controlled by manual valves, allowing the variation of the exhaust gas O_2 concentration (excess air ratio).

Around eighty percent of the flue gas is sucked by a fan via the air nozzles over ceramic honeycombs (regenerator), incorporated in the burners, for regeneration of the heat, while the remaining flue gas leaves the furnace directly via the central stack at the roof. The ratio can be varied by a manual valve installed upstream of the suction fan. During regeneration the sucked flue gas traverses the ceramic honeycomb heat exchangers situated inside the burners, while during firing mode the cold combustion air is lead over these honeycombs. Thus, the combustion air is preheated to a temperature of around 950 °C, whereas the temperature of the regenerated flue gas is approximately 150 °C, under steady state conditions.

Thermal load is simulated by a cooling system which consists of eight single ended concentric tubes, four placed at the bottom of the furnace and four at the top. Air enters the inner tube, turns at the end and flows back through the annulus. This design was made to minimize the temperature gradients along the length of the outer tube, thus, creating an as uniform as possible heat extraction distribution.

Additionally, an NDIR gas analyzer set (Sick, MAIHAK S710) monitors the flue gas after the regeneration suction fan and stack (positions ① and ② in Fig. 1, respectively) for NO and CO concentration in the flue gas. In the same position the O_2 concentration is determined paramagnetically. All the data are stored by a data acquisition system every second.

In total 18 flanges for the burners are divided over two opposite sides of the furnace (nine each). In this way, it is possible to investigate different burner configurations in the furnace. Currently, two different burners positions (Triangular and Horizontal) and for each of them two different operating modes (parallel and staggered) are being investigated. Fig. 2 shows an overview of the burner configurations. The large circles represent the burner flanges, whereas the small circles represent the location of the cooling tubes. Three burners are firing, while the other three burners are regenerating. The red filled circle represent the firing burners and the blue meshed circle represent the regenerating burners. In the unused burner flanges (blank circles) thermocouples are installed. In parallel mode three burners fire at the same side, while in staggered mode two burners fire at one side and one burner at the opposing side. After a certain time interval, all burners switch and the firing burners start regenerating and vice versa.

The three pairs of REGEMAT CD 200 B regenerative FLOX™ burners were manufactured by WS Wärmeprozesstechnik GmbH.

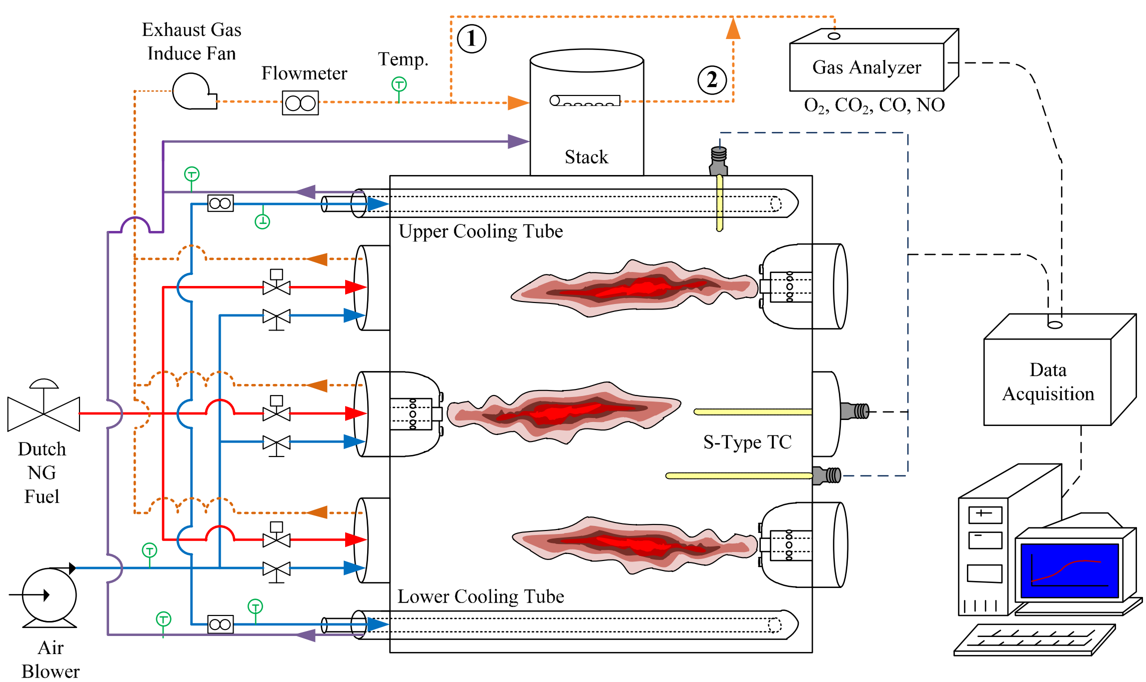

Fig. 1. Schematic diagram of the multi-burner flameless oxidation furnace.

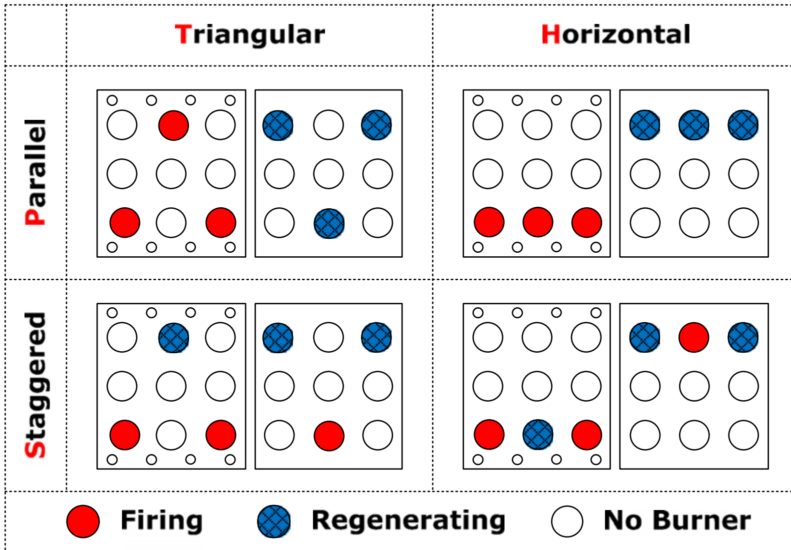

Fig. 2. Multi-burner installation map for the definition of configurations and operating modes.

Each burner has four combustion air/flue gas nozzles (d = 20 mm) around a central fuel nozzle (d = 12 mm). They can operate in two different modes and each pair has a capacity of 90/100 kW_{th} for flame and flameless condition, respectively.

Fig. 3 shows a schematic diagram and pictures of the burner firing in flame and flameless condition. In flame mode the air and fuel are premixed and the mixture is injected through the four air nozzles only. Under flameless combustion conditions the combustion air is injected through the air nozzles and the fuel is injected separately through the center fuel nozzle. During the heating up of the furnace the burners fire in flame mode. Once the furnace temperature exceeds 850 °C (this temperature is above the auto-ignition temperature of the natural gas fuel/air mixture) the burners switch to flameless firing mode automatically. Flame mode fires with a partially premixed flame and in flameless condition direct fuel injection is applied. Direct fuel injection enhances the self-recirculation of furnace burnt gas by entrainment. The fuel velocity is 30 m/s (fuel temperature is 25 °C) and the combustion air velocity is around 100 m/s (combustion air preheated to around 950 °C). Both jets are diluted by the flue gases before they meet and ignite. The reactions take place at locally low O_2 concentrations, which decreases the maximum flame temperatures and thus decrease the thermal NO_x emission.

Pictures of the combustion zones and a sketch of the jets and flame shapes for both flame and flameless conditions are presented in Fig. 3. Flame mode shows a blue premixed flame. The burners and insulations turn red during heat up. The flame disappears at the moment of transition from flame to flameless condition.

3. Mass and heat balance

Fig. 4 shows the control volume used in making the mass and heat balances over the furnace. For the different experiments, the heat and mass balances are calculated under steady state conditions. Steady state condition is assumed to be reached when the variation in the furnace temperature is almost zero with respect to time. The steady state temperature of the furnace is between 1080 °C and 1100 °C, depending on the operation parameters.

The mass balance is shown in

$$\dot{m}_{fuel} + \dot{m}_{air} = \dot{m}_{regen} + \dot{m}_{stack} \tag{1}$$

The mass flowrate of fuel ($\dot{m}_{fuel}$) and combustion air ($\dot{m}_{air}$) to the burners are monitored by measuring the differential pressure over orifice plates. During the experiments, the fuel mass flowrate is constant and the air mass flowrate is changed to change the flue

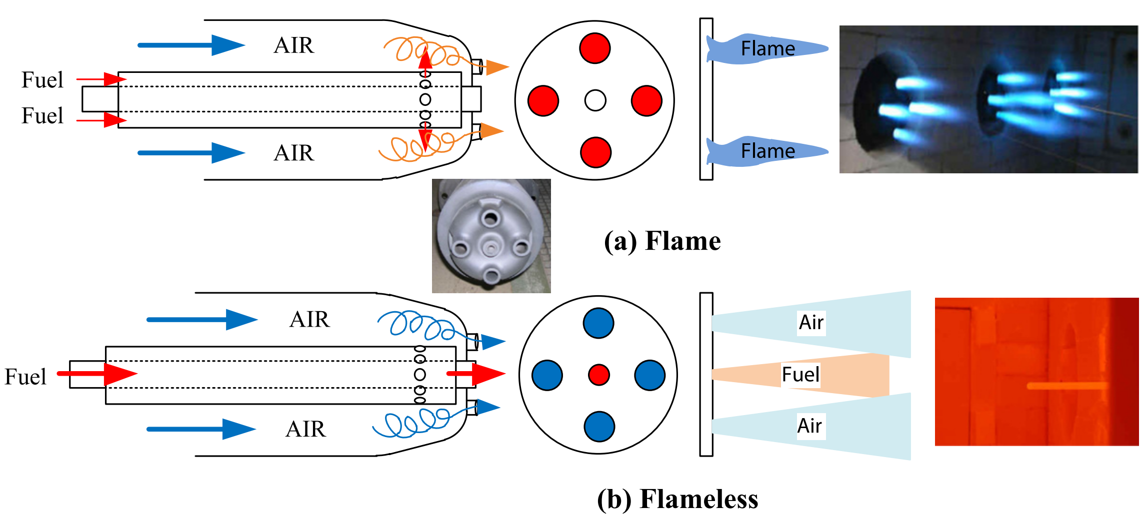

Fig. 3. Schematic diagram of a FLOX™ burner firing in flame and flameless condition.

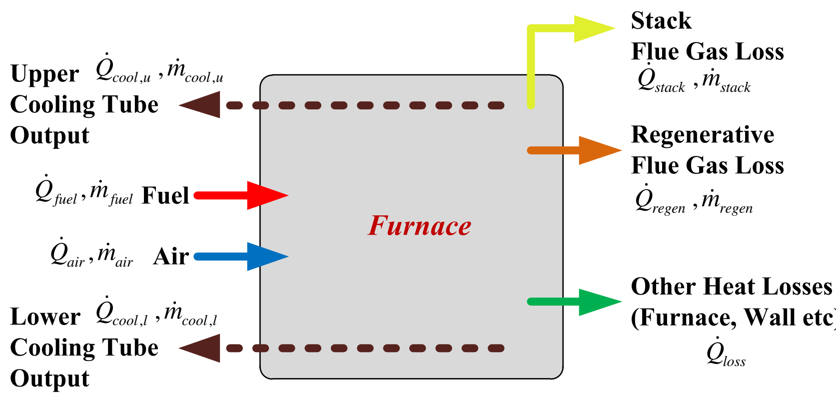

Fig. 4. Control volume of mass and heat fluxes in the flameless oxidation furnace.

gas O_2 concentration which is related to the excess air ratio (λ). The ratio of flue gas that is sucked over the regenerators ($\dot{m}_{regen}$) and that leaves the furnace via the central stack ($\dot{m}_{stack}$) can be controlled by a manual valve which is installed before the suction fan. Generally, the regenerated flue gas ($\dot{m}_{regen}$) flow is about 80%-wt of the total flue gas flow. With a vortex flow meter (KOBOLD Messring GmbH, PWL) the volume flowrate of flue gas sucked over the regenerating burners is measured and subsequently normalized with a local pressure and temperature measurement. The unknown mass flowrate of the flue gas through the stack ($\dot{m}_{stack}$) is calculated based on conservation of mass.

The cooling air mass flowrate ($\dot{m}_{cool}$) does not enter Eq. (1) since there is no mass exchange between the furnace and the heat sink. The mass flowrate of the cooling air is measured for the upper and lower cooling tubes separately with two thermal flow meters (Höntzsch, TA10).

Next, we also consider the heat balance of the furnace. For the calculation of the heat balance Eq. (2) is used.

$$\dot{Q}_{fuel} + \dot{Q}_{air} = \dot{Q}_{cool} + \dot{Q}_{regen} + \dot{Q}_{stack} + \dot{Q}_{loss} \tag{2}$$

Heat inputs are the fuel lower heating value ($\dot{Q}_{fuel}$) and the air sensible heat ($\dot{Q}_{air}$). The used fuel is Dutch natural gas. The efficiency is defined as the upper and lower cooling tube heat extraction which is calculated by measuring the air flowrate supplied to the cooling tubes and the difference between inlet and outlet temperatures. The upper and lower cooling tubes air mass flow rates are measured separately.

Losses are divided into three contributions: the first is $\dot{Q}_{regen}$, the heat in the low temperature (approx. 150 °C) flue gas exiting via the burners, the second is $\dot{Q}_{stack}$, the heat in the high temperature (approx. 1100 °C) flue gas exiting via the stack and the last is $\dot{Q}_{loss}$, the heat flux through the furnace walls and other parts. The last contribution is calculated from the heat balance. The outside wall temperature varied for different operating conditions between 60 °C and 80 °C under steady state conditions.

4. Results and discussion

4.1. Flame to flameless transition

This study is focused on flameless combustion conditions. But it is also interesting to observe the characteristics of the transition from flame to flameless during the startup of the furnace. The burner firing modes change automatically from flame to flameless when the furnace temperature is above 850 °C. Fig. 5 shows the characteristics of this transition in the horizontal parallel case. The time of zero (0) indicates the transition point.

After the transition period the slope of the furnace temperature increases under flameless combustion conditions. This shows the heat transfer enhancement based on the high momentum injection method since the flame zone spreads all around the furnace. Additionally, the fuel mass flowrate increased slightly (accompanied by a decreasing exhaust gas O_2 concentration) under flameless combustion conditions which also increases the heat transfer.

The most interesting observation is the trend in the emissions. Especially, the NO emission sharply drops under flameless combustion conditions from 80 ppm to less than 10 ppm. This is because combustion takes places in a highly diluted mixture which decreases the maximum flame temperature. NO emissions dominantly depend on the temperature. This shows that the flameless oxidation method is an effective technique to achieve low NO emissions. Also, CO emissions are decreased under flameless combustion conditions. High momentum injection enhances the fuel and air mixing which decreases the concentration of unburned products such as CO even at relatively low flame temperatures.

The experiments described hereafter concern the flameless condition. The data are collected under steady state conditions and averaged over a period of around 10 min. Whenever changing an operating condition, such as exhaust gas O_2 concentration and operating mode (parallel, staggered), care has been taken to collect data after the steady state conditions have been reestablished.

4.2. Heat balance in flameless condition

Fig. 6 shows the heat balance diagram for triangular parallel conditions. The heat input is mainly supplied by the fuel. The main portion of the heat extraction occurs by the cooling tubes (the values are range from low to high exhaust gas O_2 concentration conditions).

The efficiency of the furnace depends slightly on configurations and operating modes. However, the cooling tube efficiency decreases with an increase in the exhaust gas O_2 (46.3% → 45.2%). This decrease in efficiency is related to the increase of the combustion air mass flowrate which leads to an increase of the high temperature stack flue gas ($\dot{m}_{stack}$) mass flow rate. The regenerated flue gas ($\dot{m}_{regen}$) is almost constant regardless of the excess air ratio. Thus, the stack flue gas energy losses are increased (15.3% → 19.2%) and the furnace efficiency is lower. The decrease in the regeneration flue gas loss is relatively low (3.5% → 3.0%). Also, the furnace temperature slightly decreases with the exhaust gas O_2 concentration increasing.

Also the efficiency of the upper cooling tubes is higher than that of the lower cooling tubes. This is explained by the fact that the upper cooling tubes receive relatively more heat, by convective heat transfer, from the flue gases leaving the furnace via the stack,

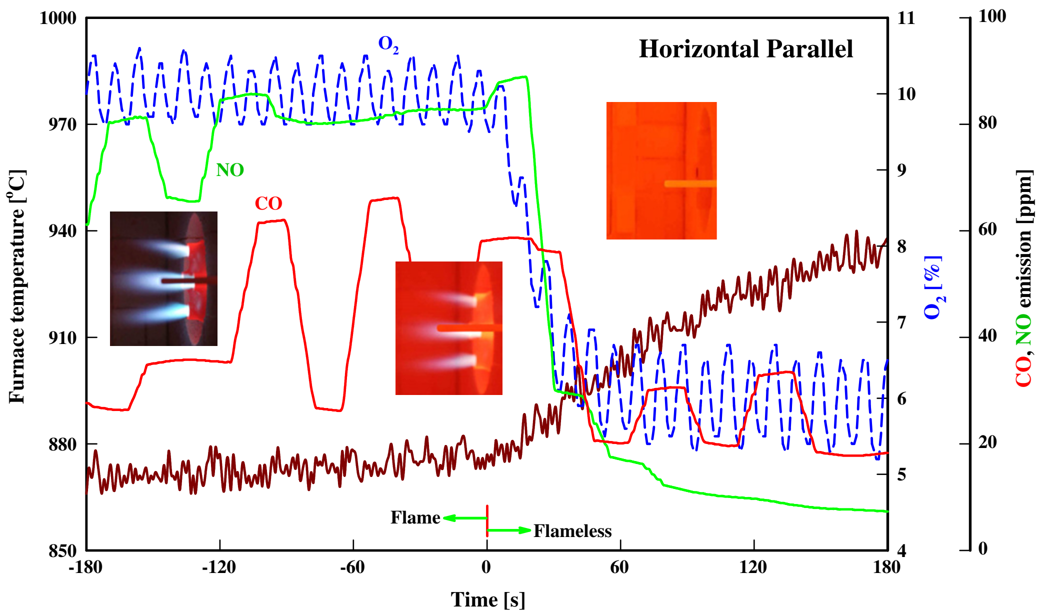

Fig. 5. Time evaluation of furnace temperature and emissions during flame to flameless transition.

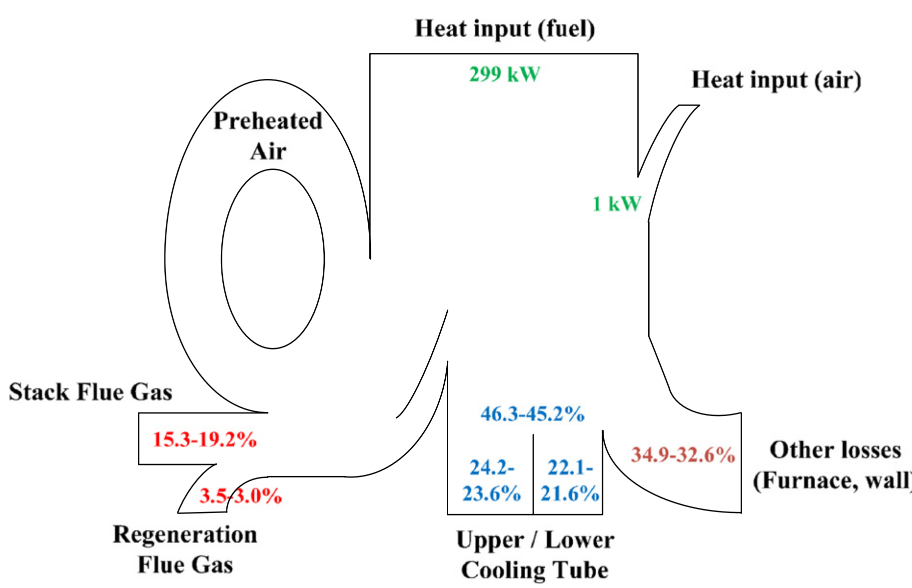

Fig. 6. Heat balance of flameless combustion conditions with excess air ratio variation in triangular parallel case.

which is situated in the roof. Buoyancy effects may also play a role. The difference is about 2%.

4.3. Temperature variations with cycle time

The variation in the furnace temperature with cycle time is shown in Fig. 7. The furnace temperature slightly increases with increasing cycle time. Also, the fluctuations in the temperature are higher for longer cycle times. Furthermore, Fig. 7 shows the temperature characteristics of the regenerator installed inside the burners. The temperature variation is increasing with longer cycle times. The maximum regenerator temperature is hardly increasing but the minimum temperature is decreasing. The temperature difference is 87 °C for a cycle time of 20 s and 105 °C of 60 s. The regenerator exit temperature is higher with longer cycle time which slightly increases the regenerative flue gas loss.

4.4. Flue gas O_2 variations with cycle time

Fig. 8 shows the time evolution of the measured composition of the flue gas after regeneration and in the stack (position ① and ② in Fig. 1) for several value of the cycle times. As mentioned before, around 80% of the flue gas exits via the regenerators and the other 20% leaves the furnace directly via the stack.

In the first part of the considered time interval the O_2 percentage was measured in the flue gas from the regenerators and in the second part, starting at about 2000s, it was measured in the flue gas from the stack. The level in the stack is clearly lower. This is due to leakage of the pneumatic valves during regeneration. When the burner is regenerating, the flue gas valve is open and the combustion air valve is closed. However, this latter valve does not close completely, as it need to leak some cold air to protect the equipment from overheating. This additional air causes the increase in

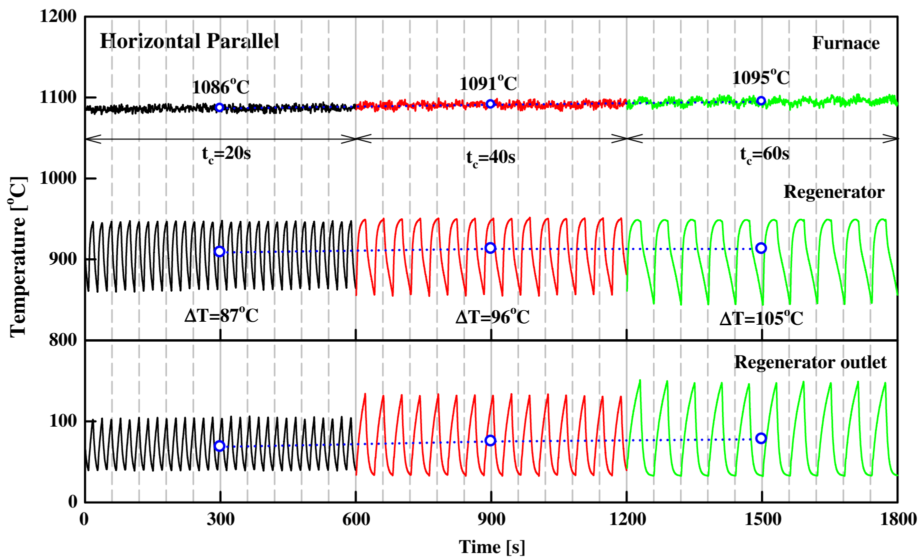

Fig. 7. Time evolution of various temperature fluctuations for cycle time variation in horizontal parallel case.

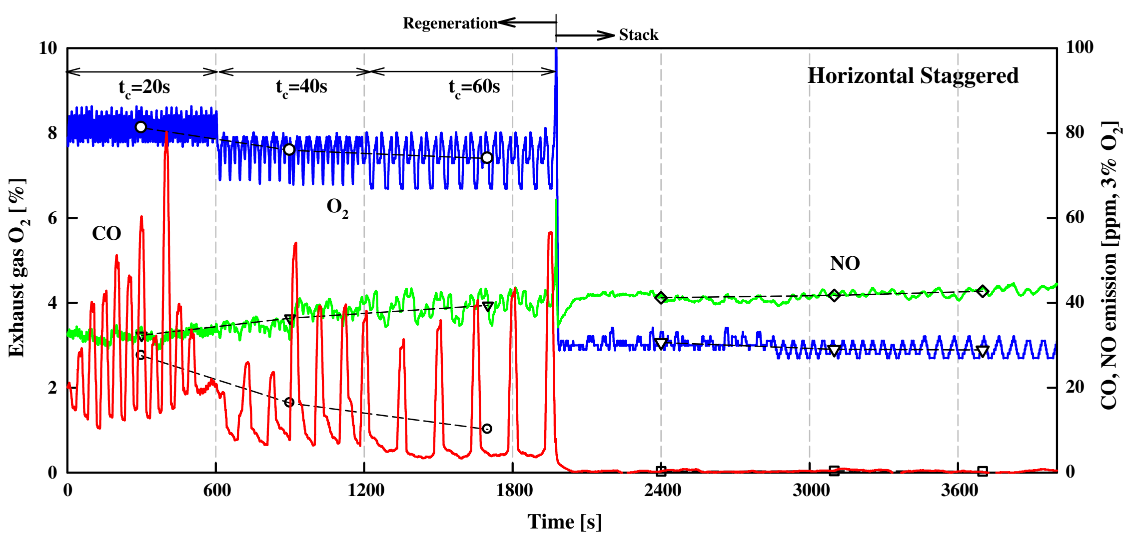

Fig. 8. Time evolution of exhaust gas O_2 and emissions for different cycle time in horizontal staggered case.

the measured O_2 concentration in the flue gas from the regenerators.

There is no CO emission measured in the stack flue gas. However, in the flue gas after regeneration CO is present. This is due to the quenching in the cold parts of the ceramic regenerators and to shorter mean path lengths to the regenerating burners and the shorter mean path lengths result in short residence time. This effect was analyzed in more detail by numerical simulation and results have been presented previously [20].

The O_2 concentration in the burner operation in furnace was made at three different cycle times (20 s, 40 s and 60 s). The averaged concentrations of O_2 and CO decrease with increasing cycle time. The frequency of CO peaks is related to the cycle time and which showed 2.5 times the cycle time. The frequency of CO peak is decrease with increasing cycle time. A subsequent closer experimental investigation using a different gas analyzer, however, has revealed that in reality there is a CO peak every cycle. For all cycle times, this second more precise measurement showed the same mean CO level as the one shown in Fig. 8. NO is slightly increasing with larger cycle time which is related to the temperature of furnace and inlet air (see in Fig. 7).

4.5. Temperature uniformity ratio

Increased temperature uniformity in the furnace is an important advantage of flameless oxidation. The spatial uniformity of the temperature in the furnace can be characterized by one variable, the temperature uniformity ratio. It is the normalized root mean square value computed from all temperature measurement and is defined in Eq. (3).

$$T_u = 1 - \sqrt{\frac{1}{N}\sum_{i=1}^{N}\left(\frac{(T_i - \overline{T})}{\overline{T}}\right)} \tag{3}$$

where T_i is the measured temperature at a certain location (i) and $\overline{T}$ is the averaged value of all measured locations in the furnace. The value of the T_u is between 0 and 1, where the value 1 indicates a perfectly uniform temperature in the furnace.

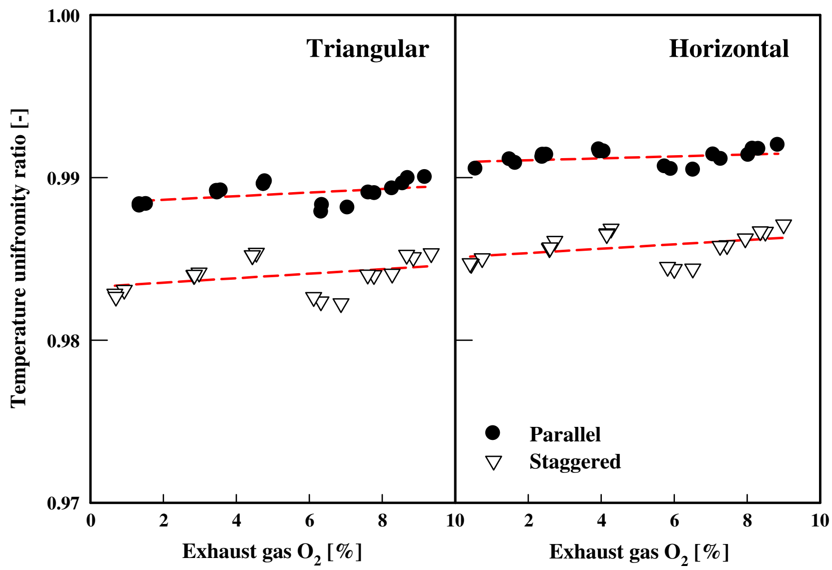

Fig. 9. Comparison of the furnace spatial temperature uniformity ratio for each configuration and firing mode.

Temperatures are measured at 18 different locations in this furnace using thermocouples type S. The thermocouples are protruding into the furnace approximately 100 mm from the inside furnace wall or via the unused burner flanges.

Fig. 9 shows the spatial temperature uniformity ratio for the two configuration and firing modes. It is observed that firing in parallel mode gives a higher temperature uniformity ratio than staggered mode. In parallel mode, three burners are firing at one side and at the other side three burners are regenerating. This leads to a more stable flow pattern inside the furnace. On the contrary, in staggered mode, the simultaneous firing burners are located on both sides. Thus the flow pattern is more complex and the flames also show impinging and merging phenomena which leads to larger temperature fluctuations. Among the parallel firing modes, the horizontal configuration shows a higher temperature uniformity ratio than triangular configuration.

4.6. Emissions

Emissions are an important criterion to identify an optimum configuration. Emissions are measured in the various cases under steady state conditions. Actually the emissions are fluctuating in time as a result of the regeneration cycle (see Fig. 8) but here we reported averaged emissions for an around 5–10 min period. NO and CO emissions were sampled both in the regeneration flue gas and in the stack flue gas.

In Fig. 10, NO and CO emissions are presented. Both the CO and NO values were recorded at different exhaust gas O_2 concentra-

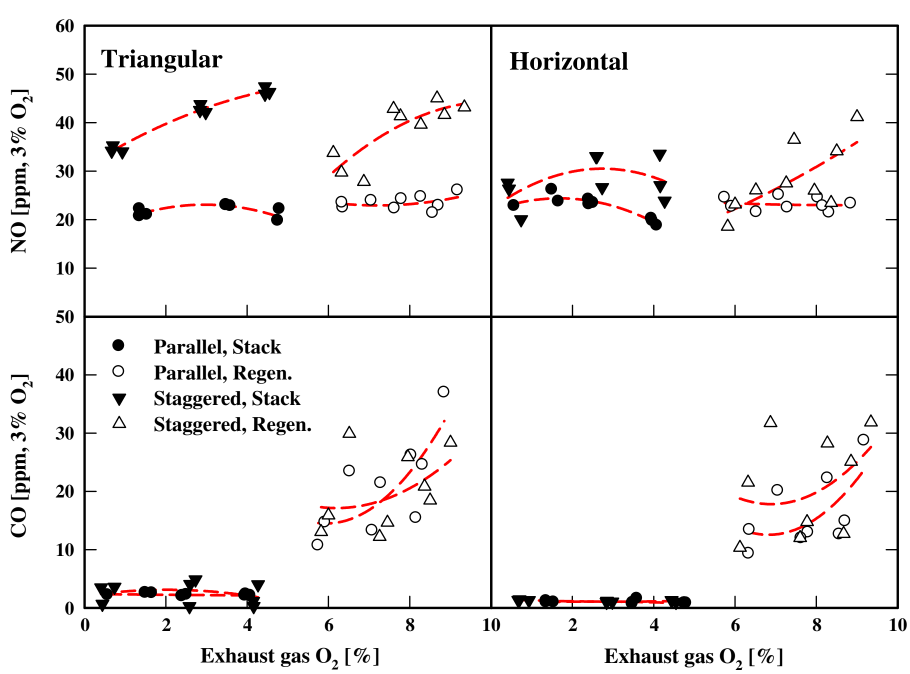

Fig. 10. NO and CO with exhaust gas O_2 at different sampling positions for each configuration and firing mode.

tions, but were subsequently normalized to 3% O_2. The values measured in the regeneration flue gas appear in the higher range of exhaust gas O_2 values, while the values from the stack flue gas appear in the lower range of exhaust gas O_2 concentrations. This is due to the air leakage previously mentioned in paragraph 4.4. The NO and CO emissions for each burner configuration and operating mode show similar trends, although there are some minor differences in local slopes.

NO emissions increase with the exhaust gas O_2, since this result in an increase in the O_2 percentage increases in the combustion zone which enhances thermal NO formation. The decrease in the NO emission at higher exhaust gas O_2 concentration due to the lowering of the flame temperature, which suppresses the thermal NO formation. Under all furnace operation condition, the measure NO concentration does not depend on whether the flue gas is sampled from the stack or after the regenerator. Apparently, parallel mode shows lower NO emission than staggered mode for all configurations. Also the horizontal configuration shows lower NO emission than the triangular configuration. This is related to the higher temperature uniformity ratio in parallel mode and horizontal configuration shown in Fig. 9. There is probably less hot spot formation in horizontal parallel mode which causes lower NO emissions.

As mentioned previously, the mean CO concentration shows different levels in the two flue gas streams. There is almost no CO measured in the stack but some CO is measured in the regeneration flue gas. In the regeneration flue gas, CO decreased slightly with increasing of exhaust gas O_2 and then increases substantially. Unlike the NO emissions, the CO emissions show only a slight difference between parallel and staggered mode. Overall, the CO emissions are below 40 ppm which is a relatively low value.

In all cases parallel firing mode shows better combustion characteristics than staggered mode. This is probably due to the fact that in parallel mode the temperature distribution is more uniform reducing NO emissions. Another factor could be the merging behavior of the jets, as observed for a furnace with four similar burners [18].

5. Concluding remarks

The characteristics of a multi-burner flameless oxidation furnace have been studied in detail for two different burner configurations and two different operating modes. The mass and heat balances were evaluated in this 300 kW_{th} three burner pair regenerative furnace. The transition from flame to flameless combustion clearly shows the merit of flameless oxidation. During flameless conditions, parallel firing mode performs better than staggered because it shows lower NO emissions for all conditions. Also, the horizontal case shows lower NO emissions. This is related to the higher temperature uniformity ratio in parallel mode and horizontal configuration. CO emissions show only a slight difference between parallel and staggered mode but the concentration is below 40 ppm which is a relatively low value.

In the future, the flame characteristics will be measured in-furnace using laser diagnostics, such as CARS and LDA for temperature and velocity measurement, respectively. These data will be used for validation of CFD simulations and design rules for multi-burner flameless oxidation furnaces will be suggested.

Acknowledgment

This Project (06910) is financially supported by the Technology Foundation STW and the Dutch Flame Foundation NVV. E-flox™ is acknowledged for giving technical support; also Dr. Wünning for his valuable advice.

References

[1] Baukal CE, Schwartz RE, editors. The John Zink combustion handbook. CRC Press; 2001.
[2] Wünning JA, Wünning JG. Flameless oxidation to reduce thermal NO-formation. Prog Energy Combust Sci 1997;23:81–94.
[3] Katsuki M, Hasegawa T. The science and technology of combustion in highly preheated air. Proc Combust Inst 1998;27:3135–46.
[4] Tsuji H, Gupta AK, Hasegawa T, Katsuki M, Kishimoto K, Morita M. High temperature air combustion. CRC Press; 2003.
[5] Özdemir ÍB, Peters N. Characteristics of the reaction zone in a combustor operating at mild combustion. Exp Fluids 2001;30:683–95.
[6] Cavaliere A, de Joannon M. Mild combustion. Prog Energy Combust Sci 2004;30:329–66.
[7] Arghode VK, Gupta AK. Development of high intensity CDC combustor for gas turbine engines. Appl Energy 2011;88:963–73.
[8] Cho E-S, Chung SH. Improvement of flame stability and NO_x reduction in hydrogen-added ultra lean premixed combustion. J Mech Sci Technol 2009;23:650–8.
[9] Milani A, Saponaro A. Diluted combustion technologies. IFRF Combust J 2001(200101).
[10] Miller JA, Bowman CT. Mechanism and modeling of nitrogen chemistry in combustion. Prog Energy Combust Sci 1989;15:287–338.
[11] Danon B, de Jong W, Roekaerts DJEM. Experimental and numerical investigation of a FLOX combust firing low calorific value gases. Combust Sci Technol 2010;88:963–73.
[12] Plessing T, Peters N, Wünning JG. Laseroptical investigation of highly preheated combustion with strong exhaust gas recirculation. Proc Combust Inst 1998;27:3197–204.
[13] Kobayashi H, Oono K, Cho E-S, Hagiwara H, Ogami Y, Niioka T. Effects of turbulence on flame structure and NO_x emission of turbulent jet non-premixed flames in high-temperature air combustion. JSME Int J 2006;48:286–92.
[14] Szegö GG, Dally BB, Nathan GJ. Operational characteristics of parallel jet MILD combustion burner system. Combust Flame 2009;156:429–38.
[15] Burggraaf BT, Lewis B, Hoppeseyn PDJ, Fricker N, Santos S, Slim BK. Toward industrial application of high efficiency combustion. IFRF Combust J 2007(200704).
[16] Yang W, Mörtberg M, Blasiak W. Influences of flame configurations on flame properties and NO emissions in combustion with high-temperature air. Scand J Metall 2005;34:7–15.
[17] Rafidi N, Blasiak W. Heat transfer characteristics of HiTAC heating furnace using regenerative burners. Appl Therm Eng 2006;26:2027–34.
[18] Danon B, Swiderski A, de Jong W, Yang W, Roekaerts DJEM. Emission and efficiency comparison of different firing modes in a furnace with four HiTAC burners. Combust Sci Technol 2011;183:686–703.
[19] Zhang C, Ishii T, Hino Y, Sugiwama S. The numerical and experimental study of non-premixed combustion flames in regenerative furnaces. J Heat Transfer 2000;122:287–93.
[20] Danon B, Cho E-S, de Jong W, Roekaerts DJEM. Carbon monoxide formation in a furnace with regenerative flameless combustion burners. In: 8th Asia pacific conference on combustion, Hyderabad, India; December 10–14, 2010.